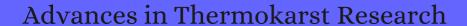
## CITATION REPORT List of articles citing



DOI: 10.1002/ppp.1779 Permafrost and Periglacial Processes, 2013, 24, 108-119.

Source: https://exaly.com/paper-pdf/55039405/citation-report.pdf

Version: 2024-04-17

This report has been generated based on the citations recorded by exaly.com for the above article. For the latest version of this publication list, visit the link given above.

The third column is the impact factor (IF) of the journal, and the fourth column is the number of citations of the article.

#	Paper	IF	Citations
290	Using Water Isotope Tracers to Develop the Hydrological Component of a Long-Term Aquatic Ecosystem Monitoring Program for a Northern Lake-Rich Landscape. <b>2013</b> , 45, 594-614		25
289	Isotropic thaw subsidence in undisturbed permafrost landscapes. <i>Geophysical Research Letters</i> , <b>2013</b> , 40, 6356-6361	4.9	60
288	Detecting Landscape Changes in High Latitude Environments Using Landsat Trend Analysis: 1. Visualization. <i>Remote Sensing</i> , <b>2014</b> , 6, 11533-11557	5	36
287	Thermokarst lake waters across the permafrost zones of western Siberia. <i>Cryosphere</i> , <b>2014</b> , 8, 1177-119	<b>93</b> 5.5	58
286	Mapping the Activity and Evolution of Retrogressive Thaw Slumps by Tasselled Cap Trend Analysis of a Landsat Satellite Image Stack. <i>Permafrost and Periglacial Processes</i> , <b>2014</b> , 25, 243-256	4.2	35
285	Variations in soil carbon dioxide efflux across a thaw slump chronosequence in northwestern Alaska. <i>Environmental Research Letters</i> , <b>2014</b> , 9, 025001	6.2	24
284	Thermokarst lakes of Western Siberia: a complex biogeochemical multidisciplinary approach. <b>2014</b> , 71, 733-748		11
283	Timing of retrogressive thaw slump initiation in the Noatak Basin, northwest Alaska, USA. <b>2014</b> , 119, 1106-1120		59
282	Effect of a thermokarst lake on soil physical properties and infiltration processes in the permafrost region of the Qinghai-Tibet Plateau, China. <b>2014</b> , 57, 2357-2365		8
281	Effects of thermo-erosion gullying on hydrologic flow networks, discharge and soil loss. <i>Environmental Research Letters</i> , <b>2014</b> , 9, 105010	6.2	41
<b>2</b> 80	Cryostratigraphy and Permafrost Evolution in the Lacustrine Lowlands of West-Central Alaska. <i>Permafrost and Periglacial Processes</i> , <b>2014</b> , 25, 14-34	4.2	53
279	Distribution and activity of ice wedges across the forest-tundra transition, western Arctic Canada. <b>2014</b> , 119, 2032-2047		40
278	Elevated dissolved organic carbon biodegradability from thawing and collapsing permafrost. <i>Journal of Geophysical Research G: Biogeosciences</i> , <b>2014</b> , 119, 2049-2063	3.7	145
277	Changes in lake area in response to thermokarst processes and climate in Old Crow Flats, Yukon. <i>Journal of Geophysical Research G: Biogeosciences</i> , <b>2015</b> , 120, 513-524	3.7	55
276	Forecasting the response of Earth's surface to future climatic and land use changes: A review of methods and research needs. <i>Earthis Future</i> , <b>2015</b> , 3, 220-251	7.9	77
275	Permafrost collapse alters soil carbon stocks, respiration, CH4, and N2O in upland tundra. <i>Global Change Biology</i> , <b>2015</b> , 21, 4570-87	11.4	112
274	Palaeoenvironmental Interpretation of Yedoma Silt (Ice Complex) Deposition as Cold-Climate Loess, Duvanny Yar, Northeast Siberia. <i>Permafrost and Periglacial Processes</i> , <b>2015</b> , 26, 208-288	4.2	73

273	Isotopic identification of soil and permafrost nitrate sources in an Arctic tundra ecosystem. <i>Journal of Geophysical Research G: Biogeosciences</i> , <b>2015</b> , 120, 1000-1017	3.7	18
272	Remote sensing measurements of thermokarst subsidence using InSAR. <b>2015</b> , 120, 1935-1948		48
271	Permafrost soils and carbon cycling. <b>2015</b> , 1, 147-171		176
270	Reviews and syntheses: Effects of permafrost thaw on Arctic aquatic ecosystems. <i>Biogeosciences</i> , <b>2015</b> , 12, 7129-7167	4.6	261
269	The role of watershed characteristics, permafrost thaw, and wildfire on dissolved organic carbon biodegradability and water chemistry in Arctic headwater streams. <i>Biogeosciences</i> , <b>2015</b> , 12, 4221-4233	4.6	51
268	Patterns and persistence of hydrologic carbon and nutrient export from collapsing upland permafrost. <i>Biogeosciences</i> , <b>2015</b> , 12, 3725-3740	4.6	120
267	The role of watershed characteristics, permafrost thaw, and wildfire on dissolved organic carbon biodegradability and water chemistry in Arctic headwater streams. <b>2015</b> ,		8
266	Methane sources in arctic thermokarst lake sediments on the North Slope of Alaska. <b>2015</b> , 13, 181-97		19
265	Extreme events in streams and rivers in arctic and subarctic regions in an uncertain future. <b>2015</b> , 60, 253	35-254	-633
264	Thermokarst lake changes between 1969 and 2010 in the Beilu River Basin, Qinghai⊞ibet Plateau, China. <b>2015</b> , 60, 556-564		46
263	Landsat-based mapping of thermokarst lake dynamics on the Tuktoyaktuk Coastal Plain, Northwest Territories, Canada since 1985. <i>Remote Sensing of Environment</i> , <b>2015</b> , 168, 194-204	13.2	45
262	High Methylmercury in Arctic and Subarctic Ponds is Related to Nutrient Levels in the Warming Eastern Canadian Arctic. <i>Environmental Science &amp; Eastern Canadian Arctic Environmental Science &amp; Eastern Canadian Environmental Environ</i>	10.3	44
261	Characterizing C-band backscattering from thermokarst lake ice on the Qinghaillibet Plateau. <i>ISPRS Journal of Photogrammetry and Remote Sensing</i> , <b>2015</b> , 104, 63-76	11.8	10
260	Evolution of the banks of thermokarst lakes in Central Yakutia (Central Siberia) due to retrogressive thaw slump activity controlled by insolation. <b>2015</b> , 241, 31-40		44
259	Increased precipitation drives mega slump development and destabilization of ice-rich permafrost terrain, northwestern Canada. <b>2015</b> , 129, 56-68		112
258	Detection and spatiotemporal analysis of methane ebullition on thermokarst lake ice using high-resolution optical aerial imagery. <i>Biogeosciences</i> , <b>2016</b> , 13, 27-44	4.6	22
257	Permafrost thaw and intense thermokarst activity decreases abundance of stream benthic macroinvertebrates. <i>Global Change Biology</i> , <b>2016</b> , 22, 2715-28	11.4	43
256	Monitoring permafrost and thermokarst processes with TanDEM-X DEM time series: Opportunities and limitations. <b>2016</b> ,		1

255	Rapid degradation of permafrost underneath waterbodies in tundra landscapes ward a representation of thermokarst in land surface models. <b>2016</b> , 121, 2446-2470		36
254	Carbon loss and chemical changes from permafrost collapse in the northern Tibetan Plateau. <i>Journal of Geophysical Research G: Biogeosciences</i> , <b>2016</b> , 121, 1781-1791	3.7	41
253	Ice processes and surface ablation in a shallow thermokarst lake in the central Qinghailibetan Plateau. <b>2016</b> , 57, 20-28		10
252	Transferability of regional permafrost disturbance susceptibility modelling using generalized linear and generalized additive models. <b>2016</b> , 264, 95-108		12
251	. <b>2016</b> , 9, 3164-3176		6
250	Spatial distribution of thermokarst terrain in Arctic Alaska. <b>2016</b> , 273, 116-133		39
249	Remote Sensing of Landscape Change in Permafrost Regions. <i>Permafrost and Periglacial Processes</i> , <b>2016</b> , 27, 324-338	4.2	55
248	Modeling and observational occurrences of near-surface drainage in Utopia Planitia, Mars. <b>2016</b> , 275, 80-89		12
247	Circumpolar distribution and carbon storage of thermokarst landscapes. <b>2016</b> , 7, 13043		238
246	Interactions of polychlorinated biphenyls and organochlorine pesticides with sedimentary organic matter of retrogressive thaw slump-affected lakes in the tundra uplands adjacent to the Mackenzie Delta, NT, Canada. <i>Journal of Geophysical Research G: Biogeosciences</i> , <b>2016</b> , 121, 411-421	3.7	12
245	Geohazards and thermal regime analysis of oil pipeline along the Qinghaillibet Plateau Engineering Corridor. <b>2016</b> , 83, 193-209		13
244	Acceleration of thaw slump activity in glaciated landscapes of the Western Canadian Arctic. <i>Environmental Research Letters</i> , <b>2016</b> , 11, 034025	6.2	77
243	From documentation to prediction: raising the bar for thermokarst research. <b>2016</b> , 24, 645-648		9
242	Spatio-Temporal Variation in High-Centre Polygons and Ice-Wedge Melt Ponds, Tuktoyaktuk Coastlands, Northwest Territories. <i>Permafrost and Periglacial Processes</i> , <b>2017</b> , 28, 66-78	4.2	23
241	The geomorphology of the Anthropocene: emergence, status and implications. <b>2017</b> , 42, 71-90		140
240	Geophysical Imaging of Permafrost and Talik Configuration Beneath a Thermokarst Lake. <i>Permafrost and Periglacial Processes</i> , <b>2017</b> , 28, 470-476	4.2	20
239	Transformation of terrestrial organic matter along thermokarst-affected permafrost coasts in the Arctic. <i>Science of the Total Environment</i> , <b>2017</b> , 581-582, 434-447	10.2	32
238	. <b>2017</b> , 10, 1687-1700		18

237	The Contribution from Methane to the Permafrost Carbon Feedback. <b>2017</b> , 3, 58-68	4
236	Climate-driven thaw of permafrost preserved glacial landscapes, northwestern Canada. <b>2017</b> , 45, 371-374	91
235	Remote sensing evaluation of High Arctic wetland depletion following permafrost disturbance by thermo-erosion gullying processes. <b>2017</b> , 3, 237-253	11
234	Inland waters and their role in the carbon cycle of Alaska. <b>2017</b> , 27, 1403-1420	51
233	Paleolimnology of thermokarst lakes: a window into permafrost landscape evolution. <b>2017</b> , 3, 91-117	41
232	Effects of warming and nitrogen fertilization on GHG flux in an alpine swamp meadow of a permafrost region. <i>Science of the Total Environment</i> , <b>2017</b> , 601-602, 1389-1399	41
231	Thermal effects of lateral supra-permafrost water flow around a thermokarst lake on the Qinghailibet Plateau. <b>2017</b> , 31, 2429-2437	9
230	Persistent Changes to Ecosystems following Winter Road Construction and Abandonment in an Area of Discontinuous Permafrost, Nahanni National Park Reserve, Northwest Territories, Canada. <b>2017</b> , 49, 259-276	3
229	Tundra vegetation stability versus lake-basin variability on the Yukon Coastal Plain (NW Canada) during the past three centuries. <b>2017</b> , 27, 1846-1858	5
228	Impacts of active retrogressive thaw slumps on vegetation, soil, and net ecosystem exchange of carbon dioxide in the Canadian High Arctic. <b>2017</b> , 3, 179-202	13
227	Large thermo-erosional tunnel for a river in northeast Greenland. <b>2017</b> , 14, 83-87	11
226	Degradation and stabilization of ice wedges: Implications for assessing risk of thermokarst in northern Alaska. <b>2017</b> , 297, 20-42	56
225	Thaw Depth Determines Dissolved Organic Carbon Concentration and Biodegradability on the Northern Qinghai-Tibetan Plateau. <i>Geophysical Research Letters</i> , <b>2017</b> , 44, 9389-9399 4-9	29
224	Terrain controls on the occurrence of coastal retrogressive thaw slumps along the Yukon Coast, Canada. <b>2017</b> , 122, 1619-1634	30
223	Linkages Among Climate, Fire, and Thermoerosion in Alaskan Tundra Over the Past Three Millennia. <i>Journal of Geophysical Research G: Biogeosciences</i> , <b>2017</b> , 122, 3362-3377	6
222	Chapter 3 Geomorphological framework: glacial and periglacial sediments, structures and landforms. <b>2017</b> , 28, 59-368	10
221	Factors influencing thermokarst lake development in Beiluhe basin, the Qinghaillibet Plateau. <b>2017</b> , 76, 1	3
220	Limnological evolution of Zelma Lake, a recently drained thermokarst lake in Old Crow Flats (Yukon, Canada). <b>2017</b> , 3, 220-236	4

219	Permafrost collapse shifts alpine tundra to a carbon source but reduces N2O and CH4 release on the northern Qinghai-Tibetan Plateau. <i>Geophysical Research Letters</i> , <b>2017</b> , 44, 8945-8952	4.9	42	
218	Retrogressive thaw slumps temper dissolved organic carbon delivery to streams of the Peel Plateau, NWT, Canada. <i>Biogeosciences</i> , <b>2017</b> , 14, 5487-5505	4.6	37	
217	Mapping permafrost landscape features using object-based image classification of multi-temporal SAR images. <i>ISPRS Journal of Photogrammetry and Remote Sensing</i> , <b>2018</b> , 141, 10-29	11.8	16	
216	The Influence of Shallow Taliks on Permafrost Thaw and Active Layer Dynamics in Subarctic Canada. <b>2018</b> , 123, 281-297		58	
215	Tundra fire alters vegetation patterns more than the resultant thermokarst. 2018, 41, 753-761		7	
214	Changes in Methane Flux along a Permafrost Thaw Sequence on the Tibetan Plateau. <i>Environmental Science &amp; Environmental Scienc</i>	10.3	31	
213	Soil organic carbon and total nitrogen pools in permafrost zones of the Qinghai-Tibetan Plateau. <b>2018</b> , 8, 3656		31	
212	Features caused by ground ice growth and decay in Late Pleistocene fluvial deposits, Paris Basin, France. <b>2018</b> , 310, 84-101		9	
211	Seasonal and multi-year surface displacements measured by DInSAR in a High Arctic permafrost environment. <b>2018</b> , 64, 51-61		23	
210	Review: Impacts of permafrost degradation on inorganic chemistry of surface fresh water. <b>2018</b> , 162, 69-83		60	
209	Impacts of Climate Change and Intensive Lesser Snow Goose (Chen caerulescens caerulescens) Activity on Surface Water in High Arctic Pond Complexes. <i>Remote Sensing</i> , <b>2018</b> , 10, 1892	5	4	
208	Permafrost Terrain Dynamics and Infrastructure Impacts Revealed by UAV Photogrammetry and Thermal Imaging. <i>Remote Sensing</i> , <b>2018</b> , 10, 1734	5	46	
207	The sign, magnitude and potential drivers of change in surface water extent in Canadian tundra. <i>Environmental Research Letters</i> , <b>2018</b> , 13, 045009	6.2	3	
206	Contrasting lake ice responses to winter climate indicate future variability and trends on the Alaskan Arctic Coastal Plain. <i>Environmental Research Letters</i> , <b>2018</b> , 13, 125001	6.2	7	
205	An estimate of ice wedge volume for a High Arctic polar desert environment, Fosheim Peninsula, Ellesmere Island. <i>Cryosphere</i> , <b>2018</b> , 12, 3589-3604	5.5	11	
204	Thermokarst pond dynamics in subarctic environment monitoring with radar remote sensing. <i>Permafrost and Periglacial Processes</i> , <b>2018</b> , 29, 231-245	4.2	4	
203	Ecological Response to Permafrost Thaw and Consequences for Local and Global Ecosystem Services. <b>2018</b> , 49, 279-301		68	
202	Biodegradability of Thermokarst Carbon in a Till-Associated, Glacial Margin Landscape: The Case of the Peel Plateau, NWT, Canada. <i>Journal of Geophysical Research G: Biogeosciences</i> , <b>2018</b> , 123, 3293-330	7 <sup>3.7</sup>	10	

201	Thaw slump activity measured using stationary cameras in time-lapse and Structure-from-Motion photogrammetry. <b>2018</b> , 4, 827-845		11
200	Effects of permafrost collapse on soil bacterial communities in a wet meadow on the northern Qinghai-Tibetan Plateau. <b>2018</b> , 18, 27		2
199	Reviews and syntheses: Changing ecosystem influences on soil thermal regimes in northern high-latitude permafrost regions. <i>Biogeosciences</i> , <b>2018</b> , 15, 5287-5313	4.6	85
198	Carbon and nitrogen pools in thermokarst-affected permafrost landscapes in Arctic Siberia. <i>Biogeosciences</i> , <b>2018</b> , 15, 953-971	4.6	28
197	Permafrost Degradation and Subsidence Observations during a Controlled Warming Experiment. <b>2018</b> , 8, 10908		10
196	Sentinel-1 InSAR Measurements of Elevation Changes over Yedoma Uplands on Sobo-Sise Island, Lena Delta. <i>Remote Sensing</i> , <b>2018</b> , 10, 1152	5	19
195	Assessment of LiDAR and Spectral Techniques for High-Resolution Mapping of Sporadic Permafrost on the Yukon-Kuskokwim Delta, Alaska. <i>Remote Sensing</i> , <b>2018</b> , 10, 258	5	10
194	Growth of Retrogressive Thaw Slumps in the Noatak Valley, Alaska, 2010\(\textit{D}\)016, Measured by Airborne Photogrammetry. <i>Remote Sensing</i> , <b>2018</b> , 10, 983	5	20
193	Sediment inputs from retrogressive thaw slumps drive algal biomass accumulation but not decomposition in Arctic streams, NWT. <b>2018</b> , 63, 1300-1315		12
192	Controls on stream hydrochemistry dynamics in a high Arctic snow-covered watershed. <b>2018</b> , 32, 3327-	3340	4
191	Methane and carbon dioxide emissions from thermokarst lakes on mineral soils. 2018, 4, 584-604		11
190	Swings in runoff at Polar Bear Pass: an extensive low-gradient wetland, Bathurst Island, Canada. <b>2019</b> , 50, 778-792		1
189	Pattern of microbial community composition and functional gene repertoire associated with methane emission from Zoige wetlands, China-A review. <i>Science of the Total Environment</i> , <b>2019</b> , 694, 133675	10.2	6
188	Using stable isotopes paired with tritium analysis to assess thermokarst lake water balances in the Source Area of the Yellow River, northeastern Qinghai-Tibet Plateau, China. <i>Science of the Total Environment</i> , <b>2019</b> , 689, 1276-1292	10.2	26
187	Revealing biogeochemical signatures of Arctic landscapes with river chemistry. <b>2019</b> , 9, 12894		31
186	High-resolution landform assemblage along a buried glacio-erosive surface in the SW Barents Sea revealed by P-Cable 3D seismic data. <b>2019</b> , 332, 33-50		14
185	Permafrost Degradation within Eastern Chukotka CALM Sites in the 21st Century Based on CMIP5 Climate Models. <b>2019</b> , 9, 232		10
184	Buried Late Weichselian thermokarst landscape discovered in the Czech Republic, central Europe. <b>2019</b> , 48, 988-1005		5

183	Pathways of ice-wedge degradation in polygonal tundra under different hydrological conditions. <i>Cryosphere</i> , <b>2019</b> , 13, 1089-1123	5.5	27
182	Thermokarst Effects on Carbon Dioxide and Methane Fluxes in Streams on the Peel Plateau (NWT, Canada). <i>Journal of Geophysical Research G: Biogeosciences</i> , <b>2019</b> , 124, 1781-1798	3.7	18
181	Rapid initialization of retrogressive thaw slumps in the Canadian high Arctic and their response to climate and terrain factors. <i>Environmental Research Letters</i> , <b>2019</b> , 14, 055006	6.2	44
180	Recent acceleration of thaw slumping in permafrost terrain of Qinghai-Tibet Plateau: An example from the Beiluhe Region. <b>2019</b> , 341, 79-85		42
179	Ecosystem changes across a gradient of permafrost degradation in subarctic QuBec (Tasiapik Valley, Nunavik, Canada). <b>2019</b> , 5, 1-26		16
178	New ground ice maps for Canada using a paleogeographic modelling approach. <i>Cryosphere</i> , <b>2019</b> , 13, 753-773	5.5	27
177	Groundwater hydrogeochemistry in permafrost regions. <i>Permafrost and Periglacial Processes</i> , <b>2019</b> , 30, 90-103	4.2	18
176	Trajectory of Topsoil Nitrogen Transformations Along a Thermo-Erosion Gully on the Tibetan Plateau. <i>Journal of Geophysical Research G: Biogeosciences</i> , <b>2019</b> , 124, 1342-1354	3.7	6
175	Identification of a Threshold Minimum Area for Reflectance Retrieval from Thermokarst Lakes and Ponds Using Full-Pixel Data from Sentinel-2. <i>Remote Sensing</i> , <b>2019</b> , 11, 657	5	11
174	Extremes of summer climate trigger thousands of thermokarst landslides in a High Arctic environment. <b>2019</b> , 10, 1329		130
174 173		3.5	130 9
	environment. <b>2019</b> , 10, 1329  Holocene Thermokarst Lake Dynamics in Northern Interior Alaska: The Interplay of Climate, Fire,	3.5	
173	environment. <b>2019</b> , 10, 1329  Holocene Thermokarst Lake Dynamics in Northern Interior Alaska: The Interplay of Climate, Fire, and Subsurface Hydrology. <i>Frontiers in Earth Science</i> , <b>2019</b> , 7,  A New Protocol to Map Permafrost Geomorphic Features and Advance Thaw-Susceptibility	3.5	9
173 172	environment. 2019, 10, 1329  Holocene Thermokarst Lake Dynamics in Northern Interior Alaska: The Interplay of Climate, Fire, and Subsurface Hydrology. Frontiers in Earth Science, 2019, 7,  A New Protocol to Map Permafrost Geomorphic Features and Advance Thaw-Susceptibility Modelling. 2019,	3.5	9
173 172 171	Holocene Thermokarst Lake Dynamics in Northern Interior Alaska: The Interplay of Climate, Fire, and Subsurface Hydrology. <i>Frontiers in Earth Science</i> , <b>2019</b> , 7,  A New Protocol to Map Permafrost Geomorphic Features and Advance Thaw-Susceptibility Modelling. <b>2019</b> ,  Determination of Communities at Risk from Thawing Permafrost. <b>2019</b> ,  Hydrometeorological measurements in peatland-dominated, discontinuous permafrost at Scotty	3.5	9
173 172 171 170	Holocene Thermokarst Lake Dynamics in Northern Interior Alaska: The Interplay of Climate, Fire, and Subsurface Hydrology. Frontiers in Earth Science, 2019, 7,  A New Protocol to Map Permafrost Geomorphic Features and Advance Thaw-Susceptibility Modelling. 2019,  Determination of Communities at Risk from Thawing Permafrost. 2019,  Hydrometeorological measurements in peatland-dominated, discontinuous permafrost at Scotty Creek, Northwest Territories, Canada. 2019, 6, 85-96  Geomorphology of Gullies at Thomas Lee Inlet, Devon Island, Canadian High Arctic. Permafrost and		9 0
173 172 171 170	Holocene Thermokarst Lake Dynamics in Northern Interior Alaska: The Interplay of Climate, Fire, and Subsurface Hydrology. <i>Frontiers in Earth Science</i> , <b>2019</b> , 7,  A New Protocol to Map Permafrost Geomorphic Features and Advance Thaw-Susceptibility Modelling. <b>2019</b> ,  Determination of Communities at Risk from Thawing Permafrost. <b>2019</b> ,  Hydrometeorological measurements in peatland-dominated, discontinuous permafrost at Scotty Creek, Northwest Territories, Canada. <b>2019</b> , 6, 85-96  Geomorphology of Gullies at Thomas Lee Inlet, Devon Island, Canadian High Arctic. <i>Permafrost and Periglacial Processes</i> , <b>2019</b> , 30, 19-34  Warming Effects of Spring Rainfall Increase Methane Emissions From Thawing Permafrost.	4.2	9 0

## (2020-2020)

165	Organic carbon stabilized by iron during slump deformation on the Qinghai-Tibetan Plateau. <i>Catena</i> , <b>2020</b> , 187, 104282	5.8	5
164	Using deep learning to map retrogressive thaw slumps in the Beiluhe region (Tibetan Plateau) from CubeSat images. <i>Remote Sensing of Environment</i> , <b>2020</b> , 237, 111534	13.2	33
163	The status and stability of permafrost carbon on the Tibetan Plateau. <i>Earth-Science Reviews</i> , <b>2020</b> , 211, 103433	10.2	33
162	Integrating isotope mass balance and water residence time dating: insights of runoff generation in small permafrost watersheds from stable and radioactive isotopes. <b>2020</b> , 326, 241-254		4
161	Transactions of the International Permafrost Association Number 3. <i>Permafrost and Periglacial Processes</i> , <b>2020</b> , 31, 343-345	4.2	
160	Assessing the Potential for Mobilization of Old Soil Carbon After Permafrost Thaw: A Synthesis of 14C Measurements From the Northern Permafrost Region. <b>2020</b> , 34, e2020GB006672		18
159	Differential impact of thermal and physical permafrost disturbances on High Arctic dissolved and particulate fluvial fluxes. <b>2020</b> , 10, 11836		12
158	Geomorphological controls over carbon distribution in permafrost soils: the case of the Narsajuaq river valley, Nunavik (Canada). <b>2020</b> , 6, 509-528		2
157	Assessment of Spatio-Temporal Landscape Changes from VHR Images in Three Different Permafrost Areas in the Western Russian Arctic. <i>Remote Sensing</i> , <b>2020</b> , 12, 3999	5	6
156	A Conceptual Model for Anticipating the Impact of Landscape Evolution on Groundwater Recharge in Degrading Permafrost Environments. <i>Geophysical Research Letters</i> , <b>2020</b> , 47, e2020GL087695	4.9	9
155	Fast response of cold ice-rich permafrost in northeast Siberia to a warming climate. <b>2020</b> , 11, 2201		65
154	Landscape matters: Predicting the biogeochemical effects of permafrost thaw on aquatic networks with a state factor approach. <i>Permafrost and Periglacial Processes</i> , <b>2020</b> , 31, 358-370	4.2	36
153	Isotopic constraints on water balance of tundra lakes and watersheds affected by permafrost degradation, Mackenzie Delta region, Northwest Territories, Canada. <i>Science of the Total Environment</i> , <b>2020</b> , 731, 139176	10.2	8
152	Carbon Thaw Rate Doubles When Accounting for Subsidence in a Permafrost Warming Experiment. <i>Journal of Geophysical Research G: Biogeosciences</i> , <b>2020</b> , 125, e2019JG005528	3.7	15
151	The Canadian Water Resource Vulnerability Index to Permafrost Thaw (CWRVIPT). <b>2020</b> , 6, 437-462		4
150	Roles of Thermokarst Lakes in a Warming World. <b>2020</b> , 28, 769-779		24
149	Specific Features of Soil Formation in Alas Landscapes of the Cryolithozone. <b>2020</b> , 90, 79-87		1
148	Post-Wildfire Surface Deformation Near Batagay, Eastern Siberia, Detected by L-Band and C-Band InSAR. <b>2020</b> , 125, e2019JF005473		10

147	A scientometric review of the research on the impacts of climate change on water quality during 1998-2018. <b>2020</b> , 27, 14322-14341		9
146	Multi-scale site evaluation of a relict active layer detachment in a High Arctic landscape. <b>2020</b> , 359, 1071	59	3
145	Lability of dissolved organic carbon from boreal peatlands: interactions between permafrost thaw, wildfire, and season. <b>2020</b> , 100, 503-515		10
144	Nitrous oxide emissions from permafrost-affected soils. <i>Nature Reviews Earth &amp; Environment</i> , <b>2020</b> , 1, 420-434	30.2	34
143	Quantifying the influence of groundwater discharge induced by permafrost degradation on lake water budget in Qinghailibet Plateau: using 222Rn and stable isotopes. <b>2020</b> , 323, 1125-1134		3
142	Microbial carbon and nitrogen processes in high-Arctic riparian soils. <i>Permafrost and Periglacial Processes</i> , <b>2020</b> , 31, 223-236	4.2	3
141	Rapid groundwater recharge dynamics determined from hydrogeochemical and isotope data in a small permafrost watershed near Umiujaq (Nunavik, Canada). <b>2020</b> , 28, 853-868		9
140	Acceleration of thaw slump during 19970017 in the Qilian Mountains of the northern Qinghai-Tibetan plateau. <b>2020</b> , 17, 1051-1062		17
139	High Arctic Vegetation Change Mediated by Hydrological Conditions. <b>2021</b> , 24, 106-121		7
138	Divergent shrub-cover responses driven by climate, wildfire, and permafrost interactions in Arctic tundra ecosystems. <i>Global Change Biology</i> , <b>2021</b> , 27, 652-663	11.4	12
137	Thermal effect of thermokarst lake on the permafrost under embankment. <b>2021</b> , 12, 76-82		2
136	Lower soil moisture and deep soil temperatures in thermokarst features increase old soil carbon loss after 10 years of experimental permafrost warming. <i>Global Change Biology</i> , <b>2021</b> , 27, 1293-1308	11.4	5
135	Retrogressive Thaw Slumps on Ice-Rich Permafrost Under Degradation: Results From a Large-Scale Laboratory Simulation. <i>Geophysical Research Letters</i> , <b>2021</b> , 48,	4.9	2
134	Spatial and stratigraphic variation of near-surface ground ice in discontinuous permafrost of the taiga shield. <i>Permafrost and Periglacial Processes</i> , <b>2021</b> , 32, 3-18	4.2	4
133	Thermokarst-like depressions on Mars: age constraints on ice degradation in Utopia Planitia. <b>2021</b> , 437-4	172	1
132	Recent thermokarst evolution in the Italian Central Alps. <i>Permafrost and Periglacial Processes</i> , <b>2021</b> , 32, 299-317	4.2	2
131	The role of liquid water in recent surface processes on Mars. <b>2021</b> , 207-261		
130	High-Latitude Rivers and Permafrost. <b>2021</b> ,		

129	Permafrost and climate change. 2021, 281-326		О
128	An Object-Based Approach for Mapping Tundra Ice-Wedge Polygon Troughs from Very High Spatial Resolution Optical Satellite Imagery. <i>Remote Sensing</i> , <b>2021</b> , 13, 558	5	3
127	Mining noise data for monitoring Arctic permafrost by using GNSS interferometric reflectometry. <b>2021</b> , 29, 100649		0
126	Degrading permafrost and its impacts. <b>2021</b> , 12, 1-5		9
125	Increasing cryospheric hazards in a warming climate. <i>Earth-Science Reviews</i> , <b>2021</b> , 213, 103500	10.2	28
124	Downstream Evolution of Particulate Organic Matter Composition From Permafrost Thaw Slumps. <i>Frontiers in Earth Science</i> , <b>2021</b> , 9,	3.5	4
123	Trends in Satellite Earth Observation for Permafrost Related Analyses A Review. <i>Remote Sensing</i> , <b>2021</b> , 13, 1217	5	6
122	Effects of multi-scale heterogeneity on the simulated evolution of ice-rich permafrost lowlands under a warming climate. <i>Cryosphere</i> , <b>2021</b> , 15, 1399-1422	5.5	4
121	Machine learning-based thermokarst landslide susceptibility modeling across the permafrost region on the Qinghai-Tibet Plateau. <b>2021</b> , 18, 2639-2649		6
120	Top-of-permafrost ground ice indicated by remotely sensed late-season subsidence. <i>Cryosphere</i> , <b>2021</b> , 15, 2041-2055	5.5	7
119	Hugh French memorial for Permafrost and Periglacial Processes. <i>Permafrost and Periglacial Processes</i> , <b>2021</b> , 32, 181-185	4.2	
118	Mapping and understanding the vulnerability of northern peatlands to permafrost thaw at scales relevant to community adaptation planning. <i>Environmental Research Letters</i> , <b>2021</b> , 16, 055022	6.2	2
117	Influence of permafrost thaw on an extreme geologic methane seep. <i>Permafrost and Periglacial Processes</i> , <b>2021</b> , 32, 484-502	4.2	1
116	Spatial Analyses and Susceptibility Modeling of Thermokarst Lakes in Permafrost Landscapes along the Qinghaillibet Engineering Corridor. <i>Remote Sensing</i> , <b>2021</b> , 13, 1974	5	3
115	Consequences of permafrost degradation for Arctic infrastructure [bridging the model gap between regional and engineering scales. <i>Cryosphere</i> , <b>2021</b> , 15, 2451-2471	5.5	11
114	Arctic wetland system dynamics under climate warming. <b>2021</b> , 8, e1526		3
113	Preferential export of permafrost-derived organic matter as retrogressive thaw slumping intensifies. <i>Environmental Research Letters</i> , <b>2021</b> , 16, 054059	6.2	7
112	Abundant and rare bacterial taxa structuring differently in sediment and water in thermokarst lakes in the Yellow River Source area, Qinghai-Tibet Plateau.		1

111	Seasonal Surface Subsidence and Frost Heave Detected by C-Band DInSAR in a High Arctic Environment, Cape Bounty, Melville Island, Nunavut, Canada. <i>Remote Sensing</i> , <b>2021</b> , 13, 2505	5	2
110	Soil macropore networks derived from X-ray computed tomography in response to typical thaw slumps in Qinghai-Tibetan Plateau, China. <b>2021</b> , 21, 2845-2854		O
109	Constraints on potential enzyme activities in thermokarst bogs: Implications for the carbon balance of peatlands following thaw. <i>Global Change Biology</i> , <b>2021</b> , 27, 4711-4726	11.4	2
108	Iron Redistribution Upon Thermokarst Processes in the Yedoma Domain. <i>Frontiers in Earth Science</i> , <b>2021</b> , 9,	3.5	2
107	Thaw-driven mass wasting couples slopes with downstream systems, and effects propagate through Arctic drainage networks. <i>Cryosphere</i> , <b>2021</b> , 15, 3059-3081	5.5	10
106	Standardized monitoring of permafrost thaw: a user-friendly, multi-parameter protocol.		О
105	Phosphorus rather than nitrogen regulates ecosystem carbon dynamics after permafrost thaw. <i>Global Change Biology</i> , <b>2021</b> , 27, 5818-5830	11.4	1
104	Recent degradation of interior Alaska permafrost mapped with ground surveys, geophysics, deep drilling, and repeat airborne lidar. <i>Cryosphere</i> , <b>2021</b> , 15, 3555-3575	5.5	7
103	Mineral Element Stocks in the Yedoma Domain: A Novel Method Applied to Ice-Rich Permafrost Regions. <i>Frontiers in Earth Science</i> , 9,	3.5	1
102	Vegetation grows more luxuriantly in Arctic permafrost drained lake basins. <i>Global Change Biology</i> , <b>2021</b> , 27, 5865-5876	11.4	4
101	Seasonal cryogenic processes control supra-permafrost pore water chemistry in two contrasting Cryosols. <b>2021</b> , 401, 115302		1
100	Seasonal deformation monitoring over thermokarst landforms using terrestrial laser scanning in Northeastern Qinghai-Tibetan Plateau. <b>2021</b> , 103, 102501		O
99	Detailed Characterization and Monitoring of a Retrogressive Thaw Slump from Remotely Piloted Aircraft Systems and Identifying Associated Influence on Carbon and Nitrogen Export. <i>Remote Sensing</i> , <b>2021</b> , 13, 171	5	3
98	Tundra wildfire triggers sustained lateral nutrient loss in Alaskan Arctic. <i>Global Change Biology</i> , <b>2021</b> , 27, 1408-1430	11.4	11
97	Mass-Movements in Cold and Polar Climates. 2021,		0
96	The Peel Plateau of Northwestern Canada: An Ice-Rich Hummocky Moraine Landscape in Transition. World Geomorphological Landscapes, <b>2017</b> , 109-122	0.4	12
95	Carbon release through abrupt permafrost thaw. <b>2020</b> , 13, 138-143		214
94	We cannot shrug off the shoulder seasons: addressing knowledge and data gaps in an Arctic headwater. <i>Environmental Research Letters</i> , <b>2020</b> , 15, 104027	6.2	20

## (2021-2020)

93	Particulate dominance of organic carbon mobilization from thaw slumps on the Peel Plateau, NT: Quantification and implications for stream systems and permafrost carbon release. <i>Environmental Research Letters</i> , <b>2020</b> , 15, 114019	6.2	16
92	Cryostratigraphical studies of ground ice formation and distribution in a High Arctic polar desert landscape, Resolute Bay, Nunavut.		1
91	Reviews and Syntheses: Effects of permafrost thaw on arctic aquatic ecosystems.		17
90	Patterns and persistence of hydrologic carbon and nutrient export from collapsing upland permafrost.		3
89	Global Positioning System interferometric reflectometry (GPS-IR) measurements of ground surface elevation changes in permafrost areas in northern Canada. <i>Cryosphere</i> , <b>2020</b> , 14, 1875-1888	5.5	3
88	Thermokarst lake inception and development in syngenetic ice-wedge polygon terrain during a cooling climatic trend, Bylot Island (Nunavut), eastern Canadian Arctic. <i>Cryosphere</i> , <b>2020</b> , 14, 2607-2627	5.5	8
87	Hydrochemical composition of thermokarst lake waters in the permafrost zone of western Siberia within the context of climate change.		1
86	Modelled present and future thaw lake area expansion/contraction trends throughout the continuous permafrost zone.		1
85	Bacterial Communities Present Distinct Co-occurrence Networks in Sediment and Water of the Thermokarst Lakes in the Yellow River Source Area. <i>Frontiers in Microbiology</i> , <b>2021</b> , 12, 716732	5.7	1
84	Status and Trends of Wetland Studies in Canada Using Remote Sensing Technology with a Focus on Wetland Classification: A Bibliographic Analysis. <i>Remote Sensing</i> , <b>2021</b> , 13, 4025	5	О
83	Sentinel-Based Inventory of Thermokarst Lakes and Ponds Across Permafrost Landscapes on the Qinghai-Tibet Plateau. <i>Earth and Space Science</i> , <b>2021</b> , 8, e2021EA001950	3.1	4
82	Detecting methane ebullition on thermokarst lake ice using high resolution optical aerial imagery.		
81	Hydrothermal processes of thermokarst ponds in the Tibetan Plateau and its thermal impact on the underlying permafrost. <i>Hupo Kexue/Journal of Lake Sciences</i> , <b>2018</b> , 30, 825-835	0.5	
80	Melville, Bathurst, and Cornwallis Islands: Low to Moderate Relief Innuitia. <i>World Geomorphological Landscapes</i> , <b>2020</b> , 315-332	0.4	
79	Remote sensing annual dynamics of rapid permafrost thaw disturbances with LandTrendr. <i>Remote Sensing of Environment</i> , <b>2022</b> , 268, 112752	13.2	2
78	Multi-Dimensional Remote Sensing Analysis Documents Beaver-Induced Permafrost Degradation, Seward Peninsula, Alaska. <i>Remote Sensing</i> , <b>2021</b> , 13, 4863	5	1
77	Methane in Zackenberg Valley, NE Greenland: multidecadal growing season fluxes of a high-Arctic tundra. <i>Biogeosciences</i> , <b>2021</b> , 18, 6093-6114	4.6	1
76	Methane emissions from northern lakes under climate change: a review. <i>SN Applied Sciences</i> , <b>2021</b> , 3, 1	1.8	Ο

75	Establishment and Verification of a Thermal Calculation Model Considering Internal Heat Transfer of Accumulated Water in Permafrost Regions. <i>Frontiers in Earth Science</i> , <b>2021</b> , 9,	3.5	O
74	Assessment of the sediment and associated nutrient/contaminant continuum, from permafrost thaw slump scars to tundra lakes in the western Canadian Arctic. <i>Permafrost and Periglacial Processes</i> ,	4.2	O
73	Identifying Barriers to Estimating Carbon Release From Interacting Feedbacks in a Warming Arctic. <i>Frontiers in Climate</i> , <b>2022</b> , 3,	7.1	0
72	Tundra vegetation change and impacts on permafrost. <i>Nature Reviews Earth &amp; Environment</i> , <b>2022</b> , 3, 68-84	30.2	11
71	The changing thermal state of permafrost. <i>Nature Reviews Earth &amp; Environment</i> , <b>2022</b> , 3, 10-23	30.2	16
70	Paleolimnological perspectives on the shifting geographic template of permafrost landscapes and its implications for Arctic freshwater biodiversity. <i>Canadian Journal of Fisheries and Aquatic Sciences</i> ,	2.4	
69	Assessing volumetric change distributions and scaling relations of retrogressive thaw slumps across the Arctic. <i>Cryosphere</i> , <b>2022</b> , 16, 1-15	5.5	3
68	Permafrost Degradation and Its Hydrogeological Impacts. Water (Switzerland), 2022, 14, 372	3	2
67	Permafrost Ground Ice Melting and Deformation Time Series Revealed by Sentinel-1 InSAR in the Tanggula Mountain Region on the Tibetan Plateau. <i>Remote Sensing</i> , <b>2022</b> , 14, 811	5	2
66	Permafrost Climate Feedbacks. <b>2022</b> , 189-209		О
65	Community Assembly and Co-Occurrence Patterns of Microeukaryotes in Thermokarst Lakes of the Yellow River Source Area <i>Microorganisms</i> , <b>2022</b> , 10,	4.9	1
64	Drivers of historical and projected changes in diverse boreal ecosystems: fires, thermokarst, riverine dynamics, and humans. <i>Environmental Research Letters</i> , <b>2022</b> , 17, 045016	6.2	О
63	Abundant and Rare Bacterial Taxa Structuring Differently in Sediment and Water in Thermokarst Lakes in the Yellow River Source Area, Qinghai-Tibet Plateau <i>Frontiers in Microbiology</i> , <b>2022</b> , 13, 77451	<b>4</b> 5·7	1
63	Abundant and Rare Bacterial Taxa Structuring Differently in Sediment and Water in Thermokarst Lakes in the Yellow River Source Area, Qinghai-Tibet Plateau <i>Frontiers in Microbiology</i> , <b>2022</b> , 13, 77451 Water body classification from high-resolution optical remote sensing imagery: Achievements and perspectives. <i>ISPRS Journal of Photogrammetry and Remote Sensing</i> , <b>2022</b> , 187, 306-327	0	4
	Lakes in the Yellow River Source Area, Qinghai-Tibet Plateau <i>Frontiers in Microbiology</i> , <b>2022</b> , 13, 77451  Water body classification from high-resolution optical remote sensing imagery: Achievements and		
62	Lakes in the Yellow River Source Area, Qinghai-Tibet Plateau <i>Frontiers in Microbiology</i> , <b>2022</b> , 13, 77451  Water body classification from high-resolution optical remote sensing imagery: Achievements and perspectives. <i>ISPRS Journal of Photogrammetry and Remote Sensing</i> , <b>2022</b> , 187, 306-327  A glimpse into the northernmost thermo-erosion gullies in Svalbard archipelago and their	11.8	4 0
62	Lakes in the Yellow River Source Area, Qinghai-Tibet Plateau <i>Frontiers in Microbiology</i> , <b>2022</b> , 13, 77451  Water body classification from high-resolution optical remote sensing imagery: Achievements and perspectives. <i>ISPRS Journal of Photogrammetry and Remote Sensing</i> , <b>2022</b> , 187, 306-327  A glimpse into the northernmost thermo-erosion gullies in Svalbard archipelago and their implications for Arctic cultural heritage. <i>Catena</i> , <b>2022</b> , 212, 106105  Sedimentary organic carbon storage of thermokarst lakes and ponds across Tibetan permafrost	11.8 5.8	4 0

57	Surface Water Dynamics and Rapid Lake Drainage in the Western Canadian Subarctic (1985\( \textbf{0}\) 2020). Journal of Geophysical Research G: Biogeosciences, <b>2021</b> , 126,	3.7	О
56	Data_Sheet_1.pdf. <b>2019</b> ,		
55	Landsat-Based Monitoring of Landscape Dynamics in Arctic Permafrost Region. <i>Journal of Remote Sensing</i> , <b>2022</b> , 2022, 1-17		2
54	Biogeography of Micro-Eukaryotic Communities in Sediment of Thermokarst Lakes Are Jointly Controlled by Spatial, Climatic, and Physicochemical Factors Across the Qinghai-Tibet Plateau. <i>Frontiers in Ecology and Evolution</i> , <b>2022</b> , 10,	3.7	0
53	Contrasting characteristics, changes, and linkages of permafrost between the Arctic and the Third Pole. <i>Earth-Science Reviews</i> , <b>2022</b> , 230, 104042	10.2	4
52	Well pads frozen foundations at the Yamburg field in a climate change. <b>2022</b> , 40-54	0.4	
51	Metagenomics Unveils Microbial Diversity and Their Biogeochemical Roles in Water and Sediment of Thermokarst Lakes in the Yellow River Source Area. <i>Microbial Ecology</i> ,	4.4	0
50	Biogeochemical Distinctiveness of Peatland Ponds, Thermokarst Waterbodies, and Lakes. <i>Geophysical Research Letters</i> , <b>2022</b> , 49,	4.9	O
49	Landslides: An emerging model for ecosystem and soil chronosequence research. <i>Earth-Science Reviews</i> , <b>2022</b> , 231, 104064	10.2	0
48	Convolutional Neural Networks for Automated Built Infrastructure Detection in the Arctic Using Sub-Meter Spatial Resolution Satellite Imagery. <i>Remote Sensing</i> , <b>2022</b> , 14, 2719	5	O
47	Divergent Trajectory of Soil Autotrophic and Heterotrophic Respiration upon Permafrost Thaw. <i>Environmental Science &amp; Environmental Science &amp; Environm</i>	10.3	0
46	Microbiome assembly in thawing permafrost and its feedbacks to climate. Global Change Biology,	11.4	1
45	Retrogressive thaw slumps in the Alaskan Low Arctic may influence tundra shrub growth more strongly than climate. <i>Ecosphere</i> , <b>2022</b> , 13,	3.1	1
44	Biogeography and environmental drivers of zooplankton communities in permafrost-affected lakes on the Qinghai-Tibet Plateau. <i>Global Ecology and Conservation</i> , <b>2022</b> , 38, e02191	2.8	1
43	We Must Stop Fossil Fuel Emissions to Protect Permafrost Ecosystems. <i>Frontiers in Environmental Science</i> , 10,	4.8	0
42	Sensitivity of erosion-rate in permafrost landscapes to changing climatic and environmental conditions based on lake sediments from Northwestern Alaska. <i>Earthis Future</i> ,	7.9	
41	Contribution of ground ice melting to the expansion of Selin Co (lake) on the Tibetan Plateau. <i>Cryosphere</i> , <b>2022</b> , 16, 2745-2767	5.5	0
40	Accelerated mobilization of organic carbon from retrogressive thaw slumps on the northern Taymyr Peninsula. <i>Cryosphere</i> , <b>2022</b> , 16, 2819-2835	5.5	O

39	Contrasted geomorphological and limnological properties of thermokarst lakes formed in buried glacier ice and ice-wedge polygon terrain. <i>Cryosphere</i> , <b>2022</b> , 16, 2837-2857	5.5	1
38	Thaw-induced impacts on land and water in discontinuous permafrost: A review of the Taiga Plains and Taiga Shield, northwestern Canada. <i>Earth-Science Reviews</i> , <b>2022</b> , 232, 104104	10.2	O
37	Abrupt increase in thermokarst lakes on the central Tibetan Plateau over the last 50 years. <i>Catena</i> , <b>2022</b> , 217, 106497	5.8	2
36	Rare bacterial biosphere is more environmental controlled and deterministically governed than abundant one in sediment of thermokarst lakes across the Qinghai-Tibet Plateau. 13,		
35	Resource limitation of autotrophs and heterotrophs in boreal forest headwater streams.		
34	Thermal effect of the accumulated water with different depths on permafrost subgrade in cold regions. <b>2022</b> ,		О
33	Understanding the change in permafrost by imaging the CRREL Permafrost Tunnel, Fairbanks, Alaska. <b>2022</b> ,		
32	Ground surface elevation changes over permafrost areas revealed by multiple GNSS interferometric reflectometry. <b>2022</b> , 96,		1
31	Rapid transformation of tundra ecosystems from ice-wedge degradation. <b>2022</b> , 216, 103921		Ο
30	Nonlinear effects of thermokarst lakes on peripheral vegetation greenness across the Qinghai-Tibet Plateau using stable isotopes and satellite detection. <b>2022</b> , 280, 113215		1
29	Metagenomic analysis reveals the diversity and distribution of antibiotic resistance genes in thermokarst lakes of the Yellow River Source Area. <b>2022</b> , 313, 120102		Ο
28	Freeze-thaw induced landslides on grasslands in cold regions. <b>2022</b> , 219, 106650		О
27	Bacterial functional redundancy and carbon metabolism potentials in soil, sediment, and water of thermokarst landscapes across the Qinghai-Tibet Plateau: Implications for the fate of permafrost carbon. <b>2022</b> , 852, 158340		О
26	TanDEM-X and Sentinel-2: Opportunities for Investigating Retrogressive Thaw Slumps. <b>2022</b> ,		О
25	Retrogressive thaw slumps along the Qinghailibet Engineering Corridor: a comprehensive inventory and their distribution characteristics. <b>2022</b> , 14, 3875-3887		1
24	Microbiogeochemical Traits to Identify Nitrogen Hotspots in Permafrost Regions. <b>2022</b> , 3, 458-501		1
23	Brief communication: Unravelling the composition and microstructure of a permafrost core using X-ray computed tomography. <b>2022</b> , 16, 3507-3515		0
22	Evidence of ground ice melting detected by InSAR and in situ monitoring over permafrost terrain on the Qinghai-Xizang (Tibet) Plateau.		O

21	Abrupt permafrost thaw accelerates carbon dioxide and methane release at a tussock tundra site. <b>2022</b> , 54, 443-464	О
20	Dynamics of Vegetation and Soil Cover of Pyrogenically Disturbed Areas of the Northern Taiga under Conditions of Thermokarst Development and Climate Warming. <b>2022</b> , 11, 1594	Ο
19	Towards Precise Drone-based Measurement of Elevation Change in Permafrost Terrain Experiencing Thaw and Thermokarst.	О
18	From permafrost soil to thermokarst lake sediment: A view from C:N:P stoichiometry. 10,	Ο
17	Changes in surface water dynamics across Northwestern Canada are influenced by wildfire and permafrost thaw.	О
16	Permafrost and Climate Change: Carbon Cycle Feedbacks From the Warming Arctic. <b>2022</b> , 47, 343-371	2
15	Landscape influence on permafrost ground ice geochemistry in a polar desert environment, Resolute Bay, Nunavut.	О
14	Sentinel responses of Arctic freshwater systems to climate: linkages, evidence, and a roadmap for future research.	O
13	Recent Intensification (2004\( \textit{1020} \)) of Permafrost Mass-Wasting in the Central Mackenzie Valley Foothills Is a Legacy of Past Forest Fire Disturbances. <b>2022</b> , 49,	О
12	Multi-hazard susceptibility mapping of cryospheric hazards in a high-Arctic environment: Svalbard Archipelago. <b>2023</b> , 15, 447-464	O
11	Using InSAR for Surface Deformation Monitoring and Active Layer Thickness Retrieval in the Heihe River Basin on the Northeast Qinghai-Tibet Plateau. <b>2023</b> , 128,	0
10	Evidence for preservation of organic carbon interacting with iron in material displaced from retrogressive thaw slumps: Case study in Peel Plateau, western Canadian Arctic. <b>2023</b> , 433, 116443	Ο
9	Remotely sensed lake area changes in permafrost regions of the Arctic and the Tibetan Plateau between 1987 and 2017. <b>2023</b> , 880, 163355	0
8	Transient Freeze-Thaw Deformation Responses to the 2018 and 2019 Fires Near Batagaika Megaslump, Northeast Siberia. <b>2023</b> , 128,	1
7	Using interferometric systhetic apparent rader (InSAR) analysis to detect ground deformation related to irreversibly changing ground ice, Mongolia.	О
6	Persistence and Potential Atmospheric Ramifications of Ice-Nucleating Particles Released from Thawing Permafrost. <b>2023</b> , 57, 3505-3515	O
5	Recognizing the Shape and Size of Tundra Lakes in Synthetic Aperture Radar (SAR) Images Using Deep Learning Segmentation. <b>2023</b> , 15, 1298	0
4	Local variability of a taiga snow cover due to vegetation and microtopography. 2023, 55,	O

Challenges in Hydrologic-Land Surface Modeling of Permafrost Signatures Canadian
Perspective. 2023, 15,

Digital Mapping of Soil Organic Carbon Using UAV Images and Soil Properties in a Thermo-Erosion
Gully on the Tibetan Plateau. 2023, 15, 1628

Hillslope erosional features and permafrost dynamics along infrastructure in the Arctic Foothills,

Alaska. 2023, 34, 208-228